

Clinical Research

Myocardial Partition Coefficient of Gadolinium: A Pilot Study in Patients With Acute Myocarditis, Chronic Myocardial Infarction, and in Healthy Volunteers

Tiago Teixeira, MD,^{a,b,*} Tarik Hafyane, MSc,^{a,*} Michael Jerosch-Herold, PhD,^c
François Marcotte, MD,^a and François-Pierre Mongeon, MD, SM^a

^a *Philippa & Marvin Carsley CMR Center, Montréal Heart Institute, Université de Montréal, Montréal, Québec, Canada*

^b *Centro Hospitalar entre Douro e Vouga, Sta Maria da Feira, Portugal*

^c *Department of Radiology, Brigham and Women's Hospital, Harvard Medical School, Boston, Massachusetts*

ABSTRACT

Background: The tissue-blood partition coefficient (PC) of gadolinium, derived from T1 measurements, reflects myocardial connective tissue fraction and tissue injury, increasing in proportion with edema or fibrosis. We determined the myocardial PC of gadolinium in patients with acute myocarditis, chronic myocardial infarction (MI), and healthy volunteers. We hypothesized that the characteristics of the injured myocardium in patients with MI and myocarditis may differ and that the PC will be higher in chronically injured myocardium (MI) compared with acutely injured myocardium (myocarditis).

Methods: We performed late gadolinium enhancement (LGE) cardiovascular magnetic resonance (CMR) imaging and T1 mapping before and after administration of gadolinium (0.1 mmol/kg Gd-BOPTA) at 3 Tesla in 10 healthy volunteers (47.1 ± 12.4 years), 18 patients with chronic MI (62.5 ± 8.1 years), and 16 patients with acute myocarditis (42.5 ± 13.9 years).

Results: In patients with chronic MI and focal scar by LGE, the whole left ventricular myocardial PC (0.45 ± 0.05) was higher compared with patients with MI without focal scar (0.39 ± 0.03, $P = 0.02$) but not significantly different from whole myocardial PC in volunteers (0.40 ± 0.05) or patients with myocarditis (0.41 ± 0.05). The PC in myocarditis scars was lower than in chronic MI scars (0.60 ± 0.12 vs

RÉSUMÉ

Introduction : Le coefficient de partage (CP) tissu/sang du gadolinium, dérivé des mesures T1, reflète la fraction de tissu conjonctif du myocarde et les lésions tissulaires, qui augmentent proportionnellement à l'œdème ou à la fibrose. Nous avons déterminé le CP du gadolinium dans le myocarde de patients atteints de myocardite aiguë, d'infarctus du myocarde (IM) chronique, et de volontaires en bonne santé. Nous avons posé l'hypothèse que les caractéristiques du myocarde lésé des patients souffrant d'IM et de myocardite peuvent être différentes et que le CP sera plus élevé dans un myocarde lésé de façon chronique que dans un myocarde lésé de façon aiguë.

Méthodes : Nous avons réalisé des séquences de rehaussement tardif après injection de gadolinium (RTG) en imagerie cardiovasculaire par résonance magnétique (IRM cardiovasculaire) et une cartographie T1 avant et après l'administration du gadolinium (Gd-BOPTA à 0,1 mmol/kg) à 3 Tesla chez 10 volontaires en bonne santé (47,1 ± 12,4 ans), 18 patients atteints d'IM chronique (62,5 ± 8,1 ans) et 16 patients atteints de myocardite aiguë (42,5 ± 13,9 ans).

Résultats : Chez les patients souffrant d'IM chronique et ayant une cicatrice focale au RTG, le CP dans le myocarde entier du ventricule gauche (0,45 ± 0,05) était plus élevé que chez les patients atteints d'IM sans cicatrice focale (0,39 ± 0,03, $P = 0,02$), mais n'était pas

Myocardial infarction (MI) and myocarditis are common causes of cardiac injury, leading to substantial morbidity and mortality.¹⁻³ MI and myocarditis may share similar clinical presentation patterns, which are difficult to differentiate using

electrocardiography (ECG),⁴ echocardiography,^{5,6} and serum markers. Cardiovascular magnetic resonance (CMR) imaging is able to characterize myocardial tissue and is the preferred noninvasive diagnostic tool for myocarditis.^{7,8} The combination of imaging myocardial edema, using water-sensitive (T2-weighted) CMR⁹ and hyperemia (early gadolinium enhancement),¹⁰ with scar imaging (late gadolinium enhancement [LGE]) has good diagnostic accuracy for myocarditis.¹¹ Furthermore, the identification of previously unrecognized myocardial infarction as areas of subendocardial scars¹² on CMR, may clarify a diagnosis of ischemic cardiomyopathy in dubious cases.

Received for publication April 14, 2018. Accepted October 10, 2018.

*These authors contributed equally to this paper.

Corresponding author: Dr François-Pierre Mongeon, Philippa & Marvin Carsley CMR Center, Montréal Heart Institute, 5000 Bélanger Street, Montréal, Québec H3T 1C1, Canada. Tel.: +1-514-376-3330; fax: +1-514-593-2158.

E-mail: francois.pierre.mongeon@umontreal.ca

See page 58 for disclosure information.

0.77 ± 0.16 , $P = 0.016$). The relationships of PC and scar burden, expressed as % LGE, were similar and significant for the 2 groups ($P = 0.042$).

Conclusion: The tissue-blood partition coefficient of Gd-BOPTA is elevated in areas of acute and chronic myocardial injury and may serve as a marker for disease activity and density of scars, which was found to be higher in chronic MI than in acute myocarditis.

Scar volume carries a prognostic value in both myocarditis and MI.¹³⁻¹⁵ Myocardial scars, however, may not have the same composition in myocarditis and MI, influenced by the extent and mechanism of the initial injury, as well as by ongoing inflammation. T2-weighted images suggest that acute myocarditis evolves from a focal to a disseminated process during the first 2 weeks, with normalization of the average myocardial signal by 12 weeks.¹⁰ In acute MI, timely reperfusion therapy limits the extension of a focal injury, as depicted by myocardial salvage, known as the difference between the area of injured myocardium by T2-weighted imaging and the final scar as defined by LGE.^{16,17} Yet, associated inflammation also takes several weeks to resolve. Furthermore, the amount of LGE undergoes dynamic changes shrinking to its chronic size during the first 8 weeks.¹⁸ The time course of these processes is only partially characterized, and scar composition is not used as a diagnostic criterion. This is partially due to limitations of current CMR techniques. The image quality of T2-weighted spin echo and early gadolinium enhancement images is often inconsistent, and the analysis of LGE images depends on the threshold used for visual assessment and recognizes focal—but not diffuse—homogeneous fibrosis.

Myocardial T1 measurement has surpassed former techniques to detect acute myocardial damage in MI^{19,20} and myocarditis²¹ and may even obviate the need for gadolinium-based contrast agents.²¹ Visual identification of irreversible injury using T1 measurements is assisted by the choice of an adequate colour scale but still requires considerable expertise. Pre- and post-contrast myocardial T1 measurements can be combined to estimate the extent of myocardial extracellular volume fraction.¹⁹ This estimation relies on calculation of the partition coefficient for gadolinium (PC), obtained by plotting the myocardial R1 (1/T1) against the blood pool R1, before and at least for 1 time point after injection of contrast material.²² The PC has been shown to be sensitive to an increased myocardial connective tissue fraction, inferring the presence of interstitial fibrosis,²³⁻²⁵ with the advantage that it relies on multiple measurements, reducing the confounders associated with post-contrast T1.

We therefore hypothesized that the characteristics of the injured myocardium in patients with MI and myocarditis will differ and that this difference can be better appreciated by calculating the PC of the scar. We hypothesize that PC will be higher in chronically injured myocardial tissue in MI compared with acutely injured tissue in myocarditis.

significativement différent du CP dans le myocarde entier des volontaires ($0,40 \pm 0,05$) ou des patients atteints de myocardite ($0,41 \pm 0,05$). Le CP dans les cicatrices de la myocardite était plus faible que celui dans les cicatrices d'IM chronique ($0,60 \pm 0,12$ vs $0,77 \pm 0,16$, $P = 0,016$). Les relations entre le CP et le fardeau des cicatrices exprimé en % de RTG étaient similaires et significatives dans les 2 groupes ($P = 0,042$).

Conclusion : Le CP tissu/sang du Gd-BOPTA s'élève dans les régions des lésions myocardiques aiguës et chroniques, et peut servir de marqueur de l'activité de la maladie et de densité des cicatrices, lequel s'est montré plus élevé lors d'IM chronique que lors de myocardite aiguë.

Materials and Methods

Study populations

Study subjects were prospectively enrolled among patients presenting for CMR at Montréal Heart Institute and were grouped as (1) suspected acute myocarditis and (2) subacute or chronic MI, depending on the clinical presentation. Patients were considered to have myocarditis (group 1) if they fulfilled the following criteria²⁶: symptoms and signs suggestive of cardiac disease (angina pectoris, dyspnea, palpitations, or fatigue) beginning in the previous 3 months; evidence of myocardial injury as defined by elevated serum markers (creatinine kinase [CK], troponin T or I) and/or ECG changes (ST-segment changes, conduction defects); exclusion of coronary artery disease either by a normal angiogram or the combination of age less than 35 years and absence of cardiovascular risk factors or a negative exercise stress test. Group 2 included outpatients, either from our institution or referred by cardiologists at other institutions, with a clinical diagnosis of MI²⁷ occurring at least 3 months before CMR referral and performing non-stress CMR as part of a long-term follow-up. However, we excluded any patient if an alternative diagnosis could clearly be suspected after integration of clinical evaluation and CMR data, even if concomitant features of MI or myocarditis were also present. Healthy volunteers were also included; these were asymptomatic individuals who volunteered for the study, who had no personal histories of cardiac disease confirmed on standardized questionnaires, and with normal left ventricular (LV) function verified after the CMR scan. We included participants between the ages of 15 and 85 years, whereas patients with hemodynamic instability, distinct histories of cardiac diseases, or known contraindications to CMR were excluded. The ethics committee approved the study, and each participant signed a written consent form.

CMR examinations

CMR examinations were performed on a 3.0 Tesla scanner (Skyra; Siemens, Erlangen, Germany), using an 18-channel phased array surface coil placed on the subject's chest. All images were ECG-gated and acquired during breath-holds. Cine images were acquired in short-axis views, covering the whole LV from above the mitral valve plane to the apex. Parameters for cine-SSFP (steady-state free precession) CMR images were field of view (FOV) 343 x 340, echo time (TE) 1.43 ms, repetition time (TR) 39.1 ms, slice thickness 8 mm

with a 2-mm gap, and 25 phases for each heart beat. The 3-3-5 Modified Look-Locker Inversion (MOLLI) recovery sequence²⁸ was used for T1 measurements with 11 SSFP readouts after inversion, slice thickness 8 mm, flip angle 35°, TE 1.07 ms, TR 371 ms, FOV 360 x 270 mm, minimum inversion time (TI) 100 ms, TI increment 80 ms, and a parallel-imaging (GRAPPA) acceleration factor of 2. MOLLI sequences were acquired in basal, mid- and apical ventricular short-axis before (native) and at 2 time points (2 to 5 and 15 minutes) after a manual intravenous injection of a single-bolus dose (0.1 mmol/kg) of Gadobenate dimeglumine (Gd-BOPTA, Multihance; Bracco, Milan, Italy). LGE images were obtained 10 to 15 minutes after injection of contrast material, in a ventricular short-axis stack, using a segmented inversion-recovery gradient-echo pulse sequence²⁹ (typical voxel size 1.4 x 1.4 x 8 mm).

CMR image analysis

All images were analyzed using clinically validated software (cvi⁴²; Circle CVI Inc, Calgary, AB). LV volumes, ejection fraction (EF), and mass were measured as per published guidelines.³⁰ The scar burden was measured as the percentage of LGE mass. For each subject, LV epi- and endocardial contours and a region of interest (ROI) in a remote myocardial segment with nulled (black) myocardium were manually drawn. A signal intensity (SI) higher than 5 standard deviations (SD) for MI or 3 SD for myocarditis above the SI of the remote area was defined as “scar,” as recommended for semiautomatic thresholding.³⁰ The resulting area within the LV myocardium was outlined as a ROI (“enhanced area”). The planimetric size of the area was transformed in volume by addition of the areas on the contiguous slices of the short-axis stack and expressed as a percentage of the myocardial surface volume (% LGE volume). We acknowledge that LGE may indicate both acute (necrosis) and chronic (fibrosis) injury; for simplicity, we used the term “scar” for both.

We measured T1 on motion-corrected³¹ SSFP MOLLI readouts; as an alternative, we used raw SSFP MOLLI readouts when image distortion caused by myocardial deformation was present on more than 3 images. To measure the T1 time in the entire myocardial surface, we used a ROI-based analysis.³² In each slice, LV epi- and endocardial contours were drawn in the first MOLLI image and forwarded to the remaining readouts to determine whole myocardium T1 measurements. Afterward, T1 was measured in the widest possible area of (1) the correspondent enhanced area of LGE images (“scar”), wherever its visual delimitation left no doubts (visually confirmed on equivalent coloured T1 maps—examples of contours shown in [Figure 1](#)), and (2) in remote nonenhanced myocardium. This allowed us to create 2 subgroups, within groups 1 and 2 based on the absence (subgroup A, example in [Figure 2](#)) or presence (subgroup B, example in [Figure 1](#)) of such an area of “scar” delineated on T1 mapping images. We rejected T1 measurements with nonsatisfactory curve fitting defined as $R^2 < 0.995$.

The gadolinium contrast partition coefficient (PC) for whole and remote myocardium, as well as for scar, was then calculated using the native and 2 post-contrast (2 to 5 and 15 minutes) T1 measurements of the referred regions. The relaxation rate ($R1 = 1/T1$) in myocardium was

plotted against the R1 in the LV blood pool. The PC was determined as the slope of the regression straight line defining the relationship between myocardial R1 vs blood pool R1.³³

Statistical analysis

Continuous variables are presented as mean \pm SD. The PC of the scar and remote myocardium was compared with a 2-tailed unpaired Students' *t*-test. Categorical variables are expressed as frequencies (percentages) and were compared using the χ^2 test. Comparisons among 3 or more groups were tested by 1-way analysis of variance (ANOVA). Post hoc pairwise comparisons were made applying a Bonferroni correction to the *P* value to account for multiple comparisons. The correlation between the percentage area of LGE and PC was calculated using a robust linear regression.³⁴ Robust linear regression was based on a generalization of maximum-likelihood estimation, based on the MM-estimator proposed by Yohai³⁵ for resistance to outliers and implemented in the MASS package for the R statistical environment.³⁶ The % LGE was modelled as a function of PC and group (MI or myocarditis) and an interaction term. A *P* value < 0.05 was considered statistically significant for all analyses. Statistical analyses were performed with SPSS version 21 (IBM, Somers, NY).

Results

Baseline characteristics

We recruited a total of 50 subjects but excluded 2 patients from the MI group and 4 patients from the myocarditis group because they presented findings consistent with other diagnoses in addition to findings suggestive of MI or myocarditis ([Supplemental Tables S1 and S2](#)). The final sample consisted of 10 healthy volunteers (80% men, 47.1 ± 12.4 years) and 34 patients: 16 with acute myocarditis (75% men, 42.5 ± 13.9 years) and 18 with subacute or chronic MI (94% men, 62.5 ± 8.1 years). Baseline characteristics and CMR data are presented in [Table 1](#). Among the 3 groups, MI patients were older, had higher prevalence of hypertension and dyslipidemia, and were more frequently taking medications known to improve LV remodelling. Per study design, patients with myocarditis were scanned closer to their event (0.49 ± 0.93 months for myocarditis vs 59.0 ± 69.5 months for MI).

Late gadolinium enhancement

LGE was absent in 22.2% (4) of MI and in 6.3% (1) of patients with acute myocarditis. All 4 patients with clinical MI diagnoses but no significant “scar” on LGE imaging had non-ST segment elevation MI (1 had very focal apical LGE beyond the location of the correspondent T1 mapping slice, and 2 others had apical mild hypokinesis without clear LGE). LGE distribution, by American Heart Association (AHA) segments, was 15% subendocardial, 7% transmural, and 2% intramural/epicardial for MI and 25% subepicardial, 11% intramural, and 2% transmural for myocarditis. The % LGE volume was not significantly different in myocarditis and in patients with chronic MI ($9.3 \pm 6.7\%$ vs $8.9 \pm 11.8\%$, $P = 0.89$). The relationships of PC and scar

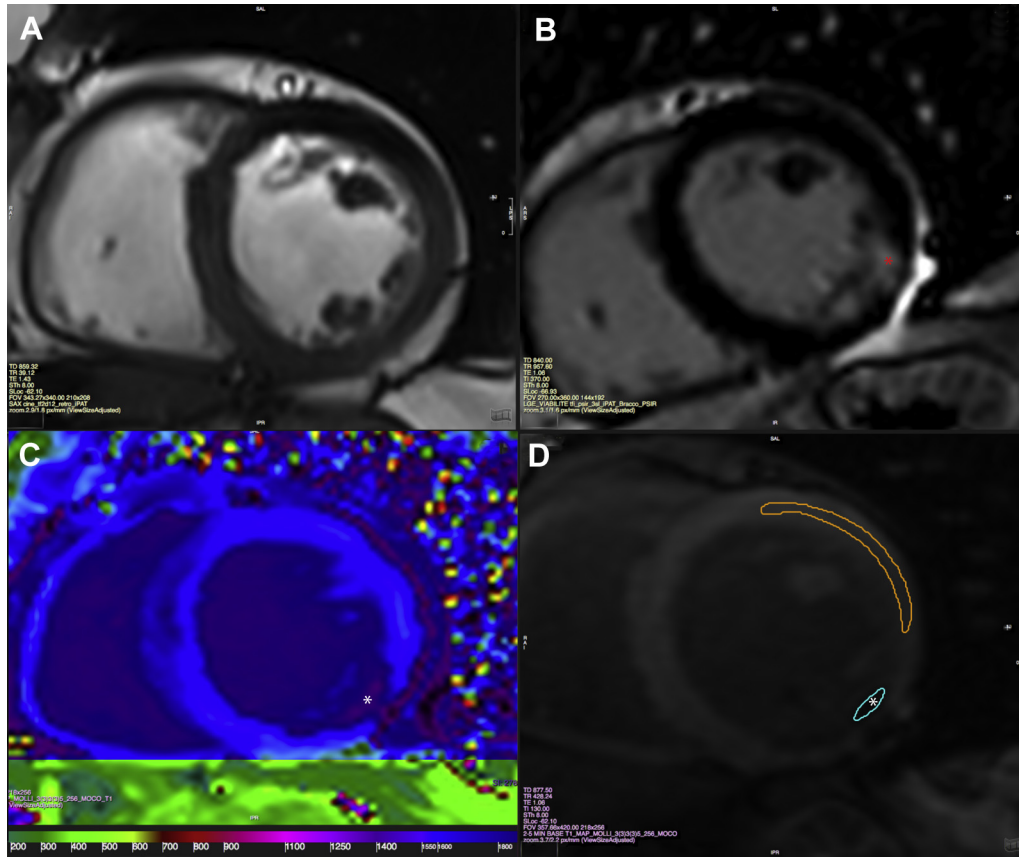


Figure 1. Tissue delineation using T1 mapping. Shown is an example of a myocardial infarction (MI) with a subendocardial scar (*) in the inferior and inferolateral segments. SSFP (A) and late gadolinium enhancement (LGE) (B) images were used for guidance. T1 color map 2 to 5 minutes post-contrast clearly identifies the scar, in purple (C). The delineation of remote myocardium and scar was possible, as illustrated in D.

burden, expressed as % LGE, were similar and significant for the 2 groups ($P = 0.042$, Fig. 3).

T1 measurements

We encountered a fair number of artifacts secondary to myocardial deformation on the motion-corrected³¹ sequences (overall excluded slices in myocarditis 8%, in MI 6%, in volunteers 3%), without statically significant differences between the different acquisition time points or among groups.

The myocardial deformation mainly presented as loss of the rounded shape of the LV, with straightening of the septum making it D-shaped.

Global native myocardial T1 was higher in myocarditis patients (1257.5 ± 61.4 ms) than in patients with MI (1211.9 ± 34.5 ms, $P = 0.05$). T1 values for each subgroup, before and after Gd-BOPTA injection, are shown in Figure 4. MI patients with “scar” (subgroup B) had lower post-contrast T1 values at 2 to 5 minutes and at 15 minutes than patients with MI without “scar” ($P < 0.01$ and $P < 0.05$ for 2 to 5

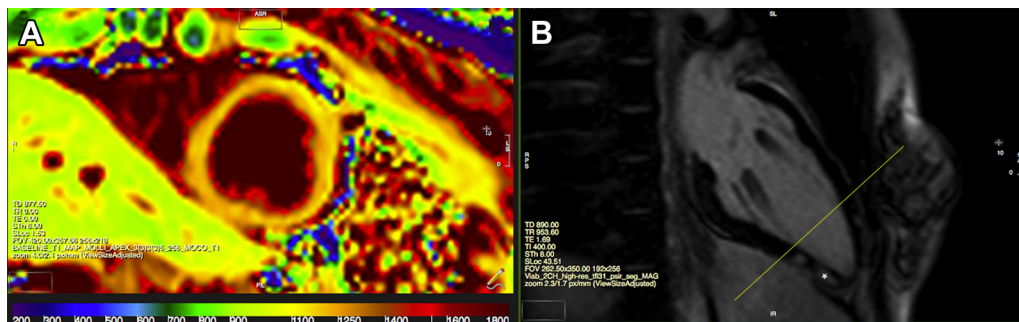


Figure 2. Example of a myocarditis patient with an apical subepicardial scar (*) on late gadolinium enhancement (LGE) images (B). However, this scar was located beyond the slice positioning for apical T1 measurements (yellow line), and therefore scar delineation was absent from native T1 color map (A), despite presence of an elevated global T1 time.

Table 1. Baseline characteristics and functional CMR values

Characteristics	Group 1 (MC)	Group 2 (MI)	<i>P</i> value	Group 3 (controls)	<i>P</i> value
N	16	18		10	
Age, years	42.5 ± 13.9	62.5 ± 8.1*		47.1 ± 12.4	< 0.001
Male sex, n (%)	12 (75)	17 (94)		8 (80)	0.28
Diabetes mellitus, n (%)	3 (18.8)	6 (33.3)	0.34	-	
Hypertension, n (%)	3 (18.8)	12 (66.7)	< 0.01	-	
Dyslipidemia, n (%)	3 (18.8)	14 (77.8)	< 0.001	-	
Family history of CAD, n (%)	4 (25)	5 (31.3)	0.69	-	
Current smoker, n (%)	2 (12.5)	5 (35.7)	0.27	-	
Time from event, months	0.49 ± 0.93	59.0 ± 69.5	< 0.001	-	
Medications					
β-Blockers, n (%)	6 (37.5)	14 (77.8)	< 0.05	-	
RAAS blockers, n (%)	4 (25)	12 (75)	< 0.01	-	
Statin, n (%)	5 (31.3)	13 (81.3)	< 0.01	-	
Antiplatelet, n (%)	7 (43.8)	16 (88.9)	< 0.01	-	
LVEDV/BSA, mL/m ²	79.8 ± 41.0	74.5 ± 19.2		89.5 ± 8.3	0.41
LVESV/BSA, mL/m ²	39.0 ± 41.7	33.5 ± 16.1		29.3 ± 6.3	0.67
LVEF, %	56.9 ± 14.4	56.6 ± 11.1		67.3 ± 6.0	0.052
LV mass/BSA, g/m ²	71.4 ± 16.5	65.5 ± 9.9		71.9 ± 13.2	0.34

BSA, body surface area; CAD, coronary artery disease; CMR, cardiovascular magnetic resonance; LVEDV, left ventricular end-diastolic volume; LVEF, left ventricular ejection fraction; LVESV, left ventricular end-systolic volume; MC, myocarditis; MI, myocardial infarction; RAAS, renin-angiotensin-aldosterone system.

*Significantly different from groups 1 and 3.

and 15 minutes post-contrast times, respectively). On visual assessment, MI T1 maps post-contrast always permitted to separate the “scar” from normal myocardium, except when it was too small (3 patients with an average % LGE of 1.3% of LV volume) or when it was located beyond the mapping slices (1 patient with septal apical infarct). Patients with myocarditis, with and without “scar” delineation on T1 maps, had similar native and post-contrast T1 values for the whole myocardial slice. Visual individualization of the “scars” on T1 maps was more difficult for myocarditis, especially because of the preferential location of the “scars” (the subepicardial border is the source of more chemical shift artifacts) and slightly more diffuse myocardial involvement.

MI and myocarditis “scars” native T1 values were higher than the native T1 of the remote myocardium. MI and myocarditis “scars” post-contrast T1 values were lower than the post-contrast T1 of the remote myocardium (Fig. 5). MI “scars” had significantly lower native and post-contrast T1 values than myocarditis “scars.”

Partition coefficient

PC results are presented in Figure 6. The whole myocardium PC was not significantly different between groups (Fig. 6A). In patients with chronic MI but not patients with myocarditis, patients with focal scar by LGE had higher whole myocardium PC than patients without focal scar (*P* = 0.02). Myocarditis scar PC was significantly lower than MI scar PC (*P* = 0.016), as seen in Figure 6B. There was no difference between remote (unscarred) myocardium PC in patients with myocarditis, patients with chronic MI, and healthy myocardium.

Discussion

Our results indicate that the PC for Gd-BOPTA of irreversibly injured myocardium was higher in MI compared with myocarditis, whereas remote myocardium was similar to the PC of myocardium in healthy volunteers. PC showed a significant association with the % volume of LGE in myocarditis and patients with chronic MI. This is consistent with previous results from histopathologic studies that correlate high collagen content with LGE.^{37,38}

We computed PC by performing MOLLI T1 measurements, before and at multiple time points after Gd-BOPTA bolus injection. Salerno et al.³⁹ validated this sequence to measure T1 and PC in volunteers, using both bolus injections and a long equilibrium infusion, without significant differences in results between both strategies. Chin et al.⁴⁰ have also shown that PC varies little over time with a wide range of T1 determinations, mainly because of the low variability of T1

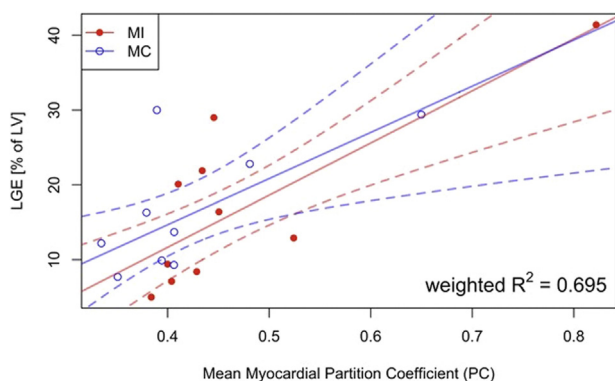


Figure 3. Scatter plot of mean myocardial partition coefficient and percentage of left ventricular volume with late gadolinium enhancement (LGE) for patients with myocarditis (MC) and myocardial infarction (MI). The linear regression lines were estimated by robust linear regression for a model with LGE as dependent variable and partition coefficient, patient group, and their interaction as predictors. The **dashed lines** delineate the 95th percentile bands for predictions. The weighted *R*² value weighs the total and residual variance in the same way that observations were weighted in the robust regression.

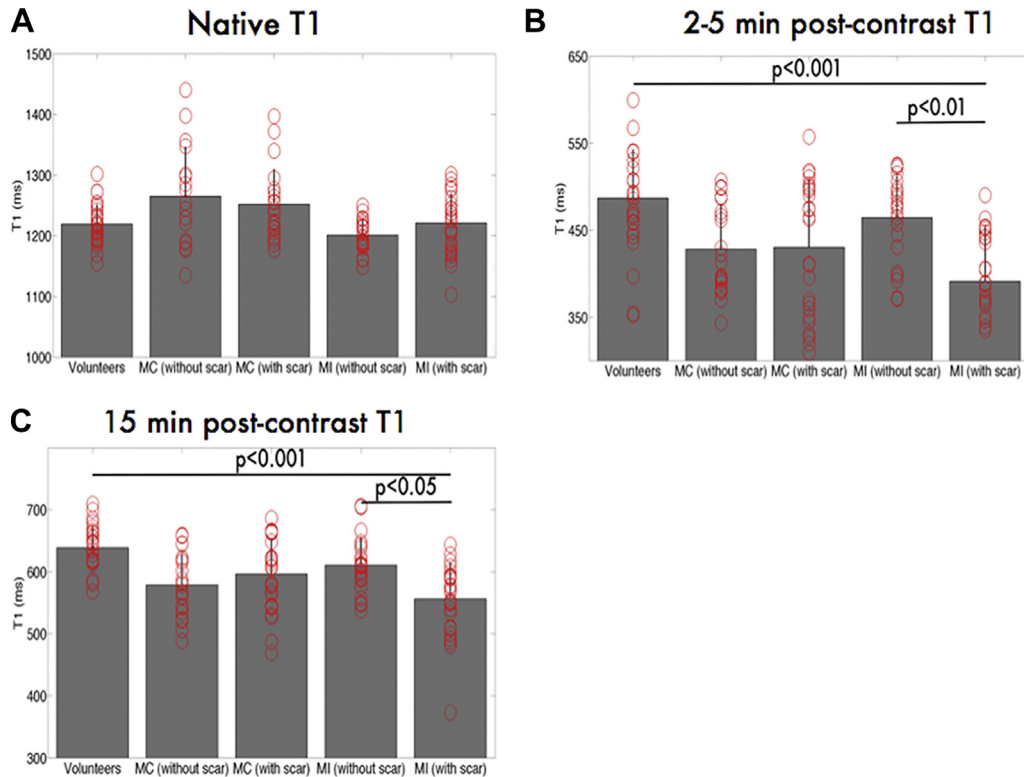


Figure 4. Global left ventricular T1 before and after Gd-BOPTA injection, (A) native T1 values, (B) 2 to 5 minutes, and (C) 15 minutes after Gd-BOPTA injection. Only significant P values ($P \leq 0.05$) are shown. Values are mean \pm standard deviation (SD).

measured beyond 15 minutes after administration of contrast material.

To confirm if PC can characterize myocardial injury, we sought to compare it with the most common noninvasive approach to detect focal irreversible myocardial injury, LGE imaging.²⁹ LGE was validated in dogs, showing an almost 1-to-1 match between the LGE areas and the histologic collagenous chronic scar.¹⁸ Based on this high concordance, the pattern of LGE can be used to differentiate pathophysiologic processes that distinctly affect myocardial muscle layers, notably MI and myocarditis.⁴¹ Furthermore, the extent of LGE has prognostic value in both diseases,¹⁵ even after controlling for EF in patients with MI.⁴² In our study, PC increased with larger “scars” and showed a significant association with % volume of LGE in the LV, in both myocarditis and patients with MI. However, computing PC may have advantages over determination of LGE extent. LGE quantification varies, depending on the method used to define enhancing myocardium: for example, the number of SD above the signal intensity of the remote myocardium or the full width-half maximum method,³⁰ without definite superiority of one technique over another.^{43,44} We used the SD method to define enhancing areas with thresholds appropriate to MI or myocarditis, as LGE evaluation criteria vary among diseases.³⁰ T1 mapping techniques are able to quantify tissue characteristics on a continuous scale, without reference to “normal” myocardium, and have an at least equivalent diagnostic performance to LGE for ischemic⁴⁵ and non-ischemic cardiomyopathies.⁴⁵ Furthermore, in diseases that diffusely affect the myocardium, such as myocarditis or

infiltrative diseases, a reference myocardial area may not be identifiable, or at least difficult to delineate, as in our patients with myocarditis, rendering the LGE technique unsuited to distinguish diseased from normal myocardium⁴⁵ and creating an advantage for T1 measurements in such cases. However, different confounders—such as the timing of acquisition after administration of contrast material, the contrast agent dose, and the washout rate—may all affect a single T1 measurement. Therefore, PC computed from all available pre- and post-contrast T1 measurements avoids most of these confounders.

The ability of PC to detect irreversible myocardial injury has been studied by Flacke et al.⁴⁶ In their study, they used a prolonged infusion of gadolinium and Look-Locker images to measure PC in healthy volunteers and patients with chronic and acute MI. PC was 0.56 in healthy myocardium compared with 0.78 in infarcted segments, a 39% difference. Our results in patients with MI also showed a difference between PC measured in MI “scar” (0.77) compared with remote myocardium (0.41), with a net difference of 88%. The PC difference in remote myocardium in these 2 studies may be related to protocol differences: namely, the sequence used or even the method of gadolinium administration. Our value of PC in healthy volunteers and remote myocardium (0.40) was closer to what has been reported by Salerno et al.³⁹ and Jerosch-Herold et al.,³³ who obtained a value of 0.45 and 0.41, respectively, using the same sequence and similar protocol. Thornhill et al.,⁴⁷ like Flacke, used a prolonged infusion of gadolinium, but with saturation recovery images to compute PC, both in a similar group of patients with MI

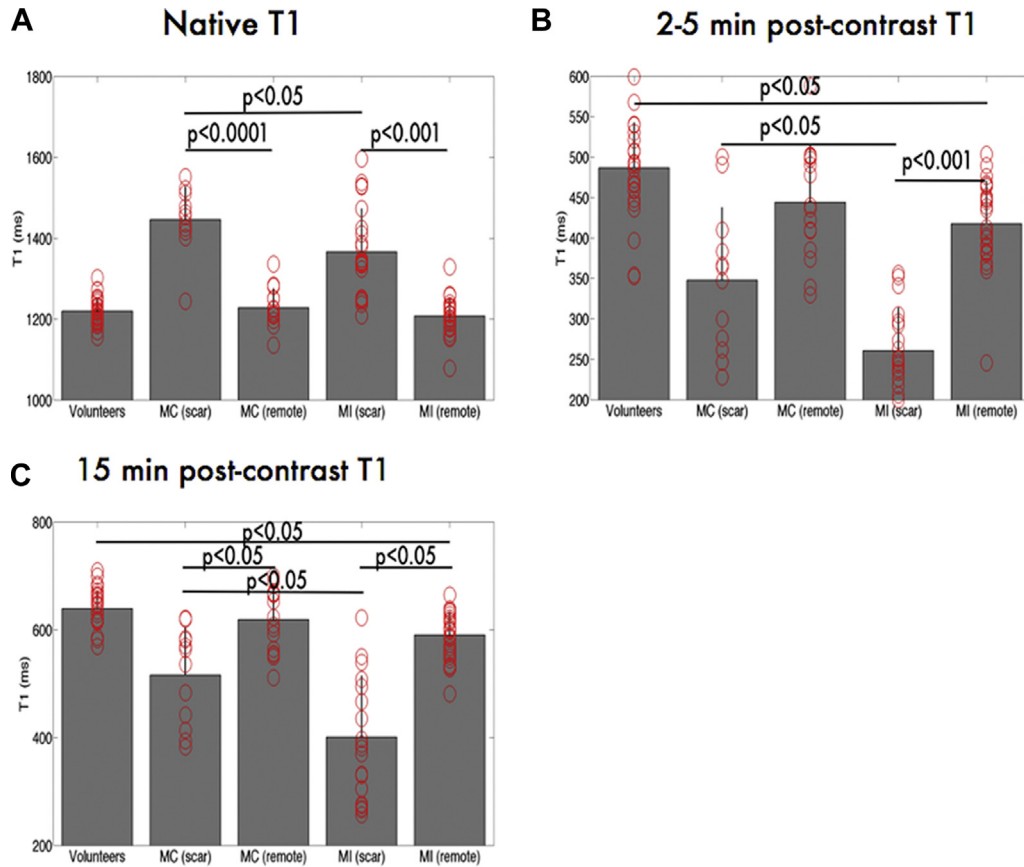


Figure 5. T1 measurements in scar tissue and remote left ventricular myocardial tissue. **(A)** Native myocardial T1, **(B)** T1 2 to 5 minutes post-contrast, and **(C)** T1 15 minutes post-contrast measured in scarred and remote left ventricular myocardium before and after Gd-BOPTA injection. Only significant P values ($P \leq 0.05$) are shown. Values are mean \pm standard deviation (SD).

during the acute (3 to 4 weeks after first event) and chronic phases (6 months after first event), as well as in healthy volunteers. However, Thornhill's estimates of normal tissue were closer to ours, at 0.46, with an elevation of 74% for PC in infarcted myocardium (0.80). Interestingly, PC did not show significant differences between the acute and chronic phases in his series.

The determination of PC in infarcted myocardial segments in the 2 previous studies^{46,47} showed no significant differences

between the acute and chronic phases of the disease. In the series by Thornhill et al., there was a small numerical difference in the PC of "scars" of distinct age, being slightly higher in the acute phase and diminishing with the evolution of the "scar." The fact that acute myocarditis "scar" already shows a lower PC (0.60) than chronic MI (0.77) suggests that the compositions of acute MC and acute/chronic MI "scars" are different, probably with less dense fibrosis and relatively more edematous tissue in myocarditis. This hypothesis is supported

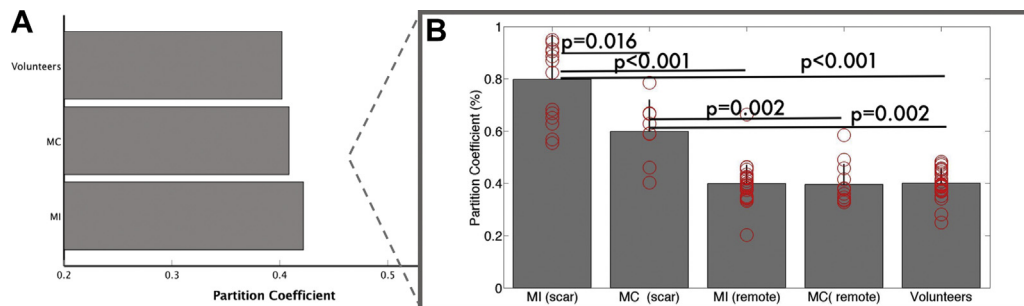


Figure 6. Partition coefficient measurements. The averages of whole myocardium PC among volunteers (0.40 ± 0.05), myocarditis (MC, 0.41 ± 0.05) and patients with myocardial infarction (MI, 0.42 ± 0.05) are shown in **A**. **(B)** We detailed the analysis, presenting comparisons of scar's and remote's myocardium PC of MI and MC patients. Scar's PC is significantly higher than the remote myocardium PC, being highest in patients with MI. Only significant P values ($P \leq 0.05$) are shown.

by a CMR follow-up study that reported an increase in myocardial contrast enhancement in the early course of MC, later decreasing at 4 weeks and returning to normal after 30 months.¹³ Our patients with myocarditis had higher native T1 values than patients with MI and healthy volunteers, which is representative of diffuse myocardial edema.

The fact that PC measured in the “scar” of myocarditis patients was significantly lower than the PC in chronic MI (0.77 ± 0.16 vs 0.60 ± 0.12 , $P = 0.016$), could therefore be used to differentiate between myocarditis and chronic MI “scars.” For clinical purposes, the usefulness of the visual recognition of the LGE pattern is unquestionable. However, myocarditis may present with multiple “scar” types, such as subendocardial location (4% in our patients with myocarditis), the extreme example being sarcoidosis, which may present with various contemporary LGE patterns. These different “scar” patterns raise the possibility of concomitant but different disease processes or, instead, of lesions with different ages. T2-weighted imaging may highlight recent lesions, but it is highly dependent on the sequence used. In our population, if one applies the myocarditis Lake Louise criteria,⁸ the diagnosis would rely solely on the LGE pattern in 93.8% of cases. However, any 2 of 3 criteria were met on 81.2% of patients, as T2-weighted imaging was only altered quantitatively in 37.5%, increasing to 75% if considering focal qualitative assessment, whereas early gadolinium enhancement was quantitatively altered also in 75%. When in doubt, the measurement of “scar” PC may help discern if different disease processes are present, based on the finding of different “scar” PCs in the same patient. The PC of an MI “scar” may be used as a reference, as it has been systematically determined around 0.8 in the different studies.^{46,47} Studies confirming the value of myocarditis “scar” PC in larger groups of patients are warranted.

Likewise, PC ability to detect diffuse extracellular volume expansion could potentially be used to monitor the progression/regression of disease, either due to fibrosis or inflammation. It has yet to be tested to monitor the response to heart failure therapies, many of which target myocardial fibrosis. Renin-angiotensin-aldosterone blockers directly prevent the development of myocardial fibrosis, improving prognosis in patients with heart failure and reduced EF.^{48,49} PC is a quantitative biomarker, with high precision, and therefore able to detect even small differences in tissue collagenous content, making it interesting for patient follow-up, especially in clinical trials. Correlations between “scar” PC and fluorodeoxyglucose uptake on positron emission tomography would also be highly informative and would be a natural next step in research, especially in cardiac sarcoidosis. However, this may prove to be a challenging experiment, as glucose metabolism by macrophages may not always allow the recognition of inflammation by fluorodeoxyglucose uptake.⁵⁰ Further studies may also test the use of PC as a diagnostic criterion for MI or myocarditis, likely in combination with other clinical or imaging parameters.

Study limitations

This feasibility study intended to apply T1 and PC determination to patients with different types of myocardial injury using high field-strength CMR. Our sample size was

small. Patients with MI and myocarditis could not be age-matched because MI and myocarditis are more prevalent in older and younger patients, respectively. Likewise, men are over-represented in our sample, also reflecting the sex distribution of patients referred for MI and myocarditis imaging. Furthermore, results may have suffered from the exclusion of myocardial segments because of insufficient image quality. Improvements in T1 measurement sequences will allow for shorter breath-holds⁵¹ and may reduce this difficulty. Our results may have gain further strength if extracellular volume fraction (ECV) could have been estimated or if histologic characterization had been possible. We could not compute the ECV because we did not possess hematocrits at the time of CMR examination for all groups of patients—namely, MI patients and volunteers—as they performed the CMR scan as outpatients. Synthetic hematocrit derived from the longitudinal relaxation of blood was proposed as new approach to compute ECV from PC when measured hematocrit is not available.⁵² However, improvements are needed, as a recent study of 114 children and young adults found that synthetic hematocrits lead to significant difference in ECV values.⁵³

Conclusions

PC of Gd-BOPTA is significantly elevated in areas of acute and chronic myocardial injury. Based on PC results, chronic MI “scars” correspond to focal areas with a higher degree of gadolinium uptake, suggesting denser focal replacement fibrosis. The longitudinal change in PC and its relation to the evolution of myocarditis should be studied as an index of disease activity.

Acknowledgements

The authors thank Matthias Friedrich, MD, and Kady Fischer, PhD, for their assistance with study design and data analysis. They also thank Dr Friedrich for his critical review of the manuscript.

Funding Sources

Funding for this study was provided by BRACCO Imaging Canada, Montreal. The Montréal Heart Institute has a research agreement with Siemens for using T1 mapping sequences.

Disclosures

The authors have no conflicts of interest to disclose.

References

- Mathers CD, Loncar D. Projections of global mortality and burden of disease from 2002 to 2030. *PLoS Med* 2006;3:e442.
- Drory Y, Turetz Y, Hiss Y, et al. Sudden unexpected death in persons less than 40 years of age. *Am J Cardiol* 1991;68:1388-92.
- Kasper EK, Agema WR, Hutchins GM, Deckers JW, Hare JM, Baughman KL. The causes of dilated cardiomyopathy: a clinicopathologic review of 673 consecutive patients. *JACC: Cardiovasc Imaging* 1994;23:586-90.

4. Liu PP, Yan AT. Cardiovascular magnetic resonance for the diagnosis of acute myocarditis: prospects for detecting myocardial inflammation. *J Am Coll Cardiol* 2005;45:1823-5.
5. Pinamonti B, Alberti E, Cigalotto A, et al. Echocardiographic findings in myocarditis. *Am J Cardiol* 1988;62:285-91.
6. Abdel-Aty H, Boyé P, Zagrosek A, et al. Diagnostic performance of cardiovascular magnetic resonance in patients with suspected acute myocarditis: comparison of different approaches. *JACC: Cardiovasc Imaging* 2005;45:1815-22.
7. Howlett JG, McKelvie RS, Arnold JMO, et al. Canadian Cardiovascular Society Consensus Conference guidelines on heart failure, update 2009: diagnosis and management of right-sided heart failure, myocarditis, device therapy and recent important clinical trials. *Can J Cardiol* 2009;25:85-105.
8. Friedrich MG, Sechtem U, Schulz-Menger J, et al. Cardiovascular magnetic resonance in myocarditis: a JACC white paper. *J Am Coll Cardiol* 2009;53:1475-87.
9. Gagliardi MG, Bevilacqua M, Di Renzi P, Picardo S, Passariello R, Marcelletti C. Usefulness of magnetic resonance imaging for diagnosis of acute myocarditis in infants and children, and comparison with endomyocardial biopsy. *Am J Cardiol* 1991;68:1089-91.
10. Friedrich MG, Strohm O, Schulz-Menger J. Contrast media-enhanced magnetic resonance imaging visualizes myocardial changes in the course of viral myocarditis. *Circulation* 1998;97:1802-9.
11. Lagan J, Schmitt M, Miller CA. Clinical applications of multi-parametric CMR in myocarditis and systemic inflammatory diseases. *Int J Cardiovasc Imaging* 2018;34:35-54.
12. McCrohon JA, Moon JCC, Prasad SK, et al. Differentiation of heart failure related to dilated cardiomyopathy and coronary artery disease using gadolinium-enhanced cardiovascular magnetic resonance. *Circulation* 2003;108:54-9.
13. Wagner A, Schulz-Menger J, Dietz R, et al. Long-term follow-up of patients with acute myocarditis by magnetic resonance imaging. *MAGMA* 2003;16:17-20.
14. Yokota H, Heidary S, Katikireddy CK, et al. Quantitative characterization of myocardial infarction by cardiovascular magnetic resonance predicts future cardiovascular events in patients with ischemic cardiomyopathy. *J Cardiovasc Magn Reson* 2008;10:17.
15. Flett AS, Westwood MA, Davies LC, Mathur A, Moon JC. The Prognostic Implications of Cardiovascular Magnetic Resonance. *Circ Cardiovasc Imaging* 2009;2:243-50.
16. Friedrich MG, Abdel-Aty H, Taylor A, Schulz-Menger J, Messroghli D, Dietz R. The salvaged area at risk in reperfused acute myocardial infarction as visualized by cardiovascular magnetic resonance. *J Am Coll Cardiol* 2008;51:1581-7.
17. Eitel I, Desch S, Fuernau G, et al. Prognostic significance and determinants of myocardial salvage assessed by cardiovascular magnetic resonance in acute reperfused myocardial infarction. *J Am Coll Cardiol* 2010;55:2470-9.
18. Kim R, Fieno D, Parrish T, et al. Relationship of MRI delayed contrast enhancement to irreversible injury, infarct age, and contractile function. *Circulation* 1999;100:1992-2002.
19. Schelbert EB, Messroghli DR. State of the art: clinical applications of cardiac T1 mapping. *Radiology* 2016;278:658-76.
20. Dall'armellina E, Piechnik SK, Ferreira VM, et al. Cardiovascular magnetic resonance by non contrast T1-mapping allows assessment of severity of injury in acute myocardial infarction. *J Cardiovasc Magn Reson* 2012;14:15.
21. Ferreira VM, Piechnik SK, Dall'armellina E, et al. Native T1-mapping detects the location, extent and patterns of acute myocarditis without the need for gadolinium contrast agents. *J Cardiovasc Magn Reson* 2014;16:36.
22. Ugander M, Oki AJ, Hsu L-Y, et al. Extracellular volume imaging by magnetic resonance imaging provides insights into overt and sub-clinical myocardial pathology. *Eur Heart J* 2012;33:1268-78.
23. Flett AS, Hayward MP, Ashworth MT, et al. Equilibrium contrast cardiovascular magnetic resonance for the measurement of diffuse myocardial fibrosis: preliminary validation in humans. *Circulation* 2010;122:138-44.
24. Iles L, Pfluger H, Phrommintikul A, et al. Evaluation of diffuse myocardial fibrosis in heart failure with cardiac magnetic resonance contrast-enhanced T1 mapping. *J Am Coll Cardiol* 2008;52:1574-80.
25. Arheden H, Saeed M, Higgins CB, et al. Measurement of the distribution volume of gadopentetate dimeglumine at echo-planar MR imaging to quantify myocardial infarction: comparison with ^{99m}Tc-DTPA autoradiography in rats. *Radiology* 1999;211:698-708.
26. Hendel RC, Friedrich MG, Schulz-Menger J, et al. CMR First-pass perfusion for suspected inducible myocardial ischemia. *JACC: Cardiovasc Imaging* 2016;9:1338-48.
27. Thygesen K, Alpert JS, Jaffe AS, et al. Third universal definition of myocardial infarction. *Eur Heart J* 2012;33:2551-67.
28. Messroghli D, Radjenovic A, Kozerke S, Higgins D, Sivanathan M, Ridgway J. Modified Look-Locker inversion recovery (MOLLI) for high-resolution T1 mapping of the heart. *Magn Reson Med* 2004;52:141-6.
29. Kim RJ, Shah DJ, Judd RM. How we perform delayed enhancement imaging. *J Cardiovasc Magn Reson* 2003;5:505-14.
30. Schulz-Menger J, Bluemke DA, Bremerich J, et al. Standardized image interpretation and post processing in cardiovascular magnetic resonance: Society for Cardiovascular Magnetic Resonance (SCMR) board of trustees task force on standardized post processing. *J Cardiovasc Magn Reson* 2013;15:35.
31. Xue H, Shah S, Greiser A, et al. Motion correction for myocardial T1 mapping using image registration with synthetic image estimation. *Magn Reson Med* 2012;67:1644-55.
32. Teixeira T, Hafyane T, Stikov N, Akdeniz C, Greiser A, Friedrich MG. Comparison of different cardiovascular magnetic resonance sequences for native myocardial T1 mapping at 3T. *J Cardiovasc Magn Reson* 2016;18:65.
33. Jerosch-Herold M, Sheridan DC, Kushner JD, et al. Cardiac magnetic resonance imaging of myocardial contrast uptake and blood flow in patients affected with idiopathic or familial dilated cardiomyopathy. *Am J Physiol Heart Circ Physiol* 2008;295:H1234-42.
34. Li G. Robust regression. In: Hoaglin DC, Mosteller F, Tukey JW, eds. *Exploring Data Tables, Trends and Shapes*. New York: Wiley; 1985.
35. Yohai VJ. High breakdown-point and high efficiency robust estimates for regression. *Ann Stat* 1987;15:642-56.
36. Venables WN, Ripley BD. *Modern Applied Statistics With S*. 4th ed. New York, NY: Springer; 2002:156-8.
37. Moon JCC, Reed E, Sheppard MN, et al. The histologic basis of late gadolinium enhancement cardiovascular magnetic resonance in hypertrophic cardiomyopathy. *JACC: Cardiovasc Imaging* 2004;43:2260-4.

38. Moravsky G, Ofek E, Rakowski H, et al. Myocardial fibrosis in hypertrophic cardiomyopathy: accurate reflection of histopathological findings by CMR. *JACC: Cardiovasc Imaging* 2013;6:587-96.
39. Salerno M, Janardhanan R, Jiji RS, et al. Comparison of methods for determining the partition coefficient of gadolinium in the myocardium using T1 mapping. *J Magn Reson Imaging* 2013;38:217-24.
40. Chin CWL, Semple S, Malley T, et al. Optimization and comparison of myocardial T1 techniques at 3T in patients with aortic stenosis. *Eur Heart J Cardiovasc Imaging* 2013;15:556-65.
41. Mahrholdt H. Delayed enhancement cardiovascular magnetic resonance assessment of non-ischaemic cardiomyopathies. *Eur Heart J* 2005;26:1461-74.
42. Wu E, Ortiz JT, Tejedor P, et al. Infarct size by contrast enhanced cardiac magnetic resonance is a stronger predictor of outcomes than left ventricular ejection fraction or end-systolic volume index: prospective cohort study. *Heart* 2008;94:730-6.
43. Flett AS, Hasleton J, Cook C, et al. Evaluation of techniques for the quantification of myocardial scar of differing etiology using cardiac magnetic resonance. *JACC: Cardiovasc Imaging* 2011;4:150-6.
44. Spiewak M, Malek LA, Misko J, et al. Comparison of different quantification methods of late gadolinium enhancement in patients with hypertrophic cardiomyopathy. *Eur J Radiol* 2010;74:e149-53.
45. Ferreira VM, Piechnik SK, Dall'armellina E, et al. Non-contrast T1-mapping detects acute myocardial edema with high diagnostic accuracy: a comparison to T2-weighted cardiovascular magnetic resonance. *J Cardiovasc Magn Reson* 2012;14:42.
46. Flacke SJ, Fischer SE, Lorenz CH. Measurement of the gadopentetate dimeglumine partition coefficient in human myocardium in vivo: normal distribution and elevation in acute and chronic infarction. *Radiology* 2001;218:703-10.
47. Thornhill RE, Prato FS, Wisenberg G, White JA, Nowell J, Sauer A. Feasibility of the single-bolus strategy for measuring the partition coefficient of Gd-DTPA in patients with myocardial infarction: independence of image delay time and maturity of scar. *Magn Reson Med* 2006;55:780-9.
48. Dzaou VJ, Antman EM, Black HR, et al. The cardiovascular disease continuum validated: clinical evidence of improved patient outcomes: part I: Pathophysiology and clinical trial evidence (risk factors through stable coronary artery disease). *Circulation* 2006;114:2850-70.
49. O'Rourke MF, Safar ME, Dzaou V. The cardiovascular continuum extended: aging effects on the aorta and microvasculature. *Vasc Med* 2010;15:461-8.
50. Tavakoli S, Zamora D, Ullevig S, Asmis R. Bioenergetic profiles diverge during macrophage polarization: implications for the interpretation of 18F-FDG PET imaging of atherosclerosis. *J Nucl Med* 2013;54:1661-7.
51. Piechnik SK, Ferreira VM, Dall'armellina E, et al. Shortened Modified Look-Locker Inversion recovery (ShMOLLI) for clinical myocardial T1-mapping at 1.5 and 3 T within a 9 heartbeat breathhold. *J Cardiovasc Magn Reson* 2010;12:69.
52. Treibel TA, Fontana M, Maestrini V, et al. Automatic measurement of the myocardial interstitium: synthetic extracellular volume quantification without hematocrit sampling. *JACC: Cardiovasc Imaging* 2016;9:54-63.
53. Raucic FJ, Parra DA, Christensen JT, et al. Synthetic hematocrit derived from the longitudinal relaxation of blood can lead to clinically significant errors in measurement of extracellular volume fraction in pediatric and young adult patients. *J Cardiovasc Magn Reson* 2017;19:58.

Supplementary Material

To access the supplementary material accompanying this article, visit the online version of *Canadian Journal of Cardiology* at www.onlinecjc.ca and at <https://doi.org/10.1016/j.cjca.2018.10.005>.